

Fatigue life assessment of steel connectors in the adjustable column-base connection for high-speed rail

Piotr KOZIOL *

Wrocław University of Science and Technology, Faculty of Civil Engineering,
Wybrzeże Wyspiańskiego 27, 50-370 Wrocław, Poland

Abstract. High-speed rail (HSR) systems provide numerous benefits, including reduced travel time, increased transport capacity, and lower environmental impact compared to conventional rail networks. Recent experience in Poland has confirmed that the design of high-speed rail lines requires the development of new, dedicated structural solutions. One such example is the need to assess the load-bearing capacity of the column-to-foundation connection, which in Poland is designed as a connection with a spacing between the column base plate and the top part of the pile foundation – an uncommon solution in HSR applications. The study included the development of a fatigue damage spectrum in the high-cycle range, taking into account stress variability caused by pressure fluctuations from passing trains. The results establish a relationship between the number of load cycles and pressure values, enabling a simplified estimation of the fatigue strength of the examined connection. Wind effects are influenced by several factors, including train speed, aerodynamic shape, and the angle of load application. The study highlights the sensitivity of the system to boundary conditions and recommends design improvements to enhance fatigue resistance. The novelty of the work lies in identifying critical failure modes specific to distance-type connections and emphasizing the need for full-scale experimental validation in the context of HSR development in Poland.

Keywords: adjustable connection; bolt; fatigue life; life prediction; high-speed rail.

1. INTRODUCTION

High-speed rail (HSR) (Fig. 1) is currently one of the fastest-growing sectors of infrastructure. It is particularly important for society as it can significantly improve travel comfort, reduce journey times between cities, and contribute to lowering CO₂ emissions. Enhancing the reliability and quality of rail transport



Fig. 1. HSR – Shinkansen bullet train in Japan

relieves road and air infrastructure, connects different regions of the country, and reduces travel costs. HSR is one of the safest and most cost-effective means of transportation. Railway infrastructure is also considered critical, playing a fundamental role for the country in both civilian and military aspects. Therefore, ensuring its reliability requires continuous financial investment not only in the maintenance of the existing railway network but also in its systematic expansion, with particular emphasis on the development of HSR. In this process, special attention must be paid to the durability of components that are already in service. Existing traction poles, for example, require regular assessment of their technical condition and appropriate maintenance measures to ensure guarantee safe and long-term operation [1]. At the same time, when entirely new HSR lines are designed, the challenge shifts from maintaining existing infrastructure to creating optimized solutions. This requires the use of advanced computational methods supported by research [2,3], which results in the optimization of both the structural elements and their foundations. Apart from economic and social considerations, one of the important technical barriers to implementing HSR solutions for the first time in a specific country is the lack of structural solutions that ensure the safe and durable operation of the railway line.

HSR refers to lines that enable speeds of 250 km/h or higher on newly constructed tracks (and above 200 km/h on modernized tracks), along with rolling stock that meets these requirements [4].

*e-mail: piotr.koziol@pwr.edu.pl

Manuscript submitted 2025-03-31, revised 2025-06-10, initially accepted for publication 2025-06-10, published in August 2025.

1.1. Structural requirements for overhead line equipment masts

The design of HSR differs from traditional railways, not only in terms of the performance of the rolling stock. High-speed rolling stock requires appropriate track geometry (such as larger curve radius, lower track gradients), increased bearing capacity of the embankment and subsoil (including higher strength, stability, and adapted drainage), as well as a dedicated supporting structure for the traction network (such as higher power supply capacities and increased train speeds), among other things. The final solution is the result of all these factors. This article focuses solely on the safety of the supporting structure for overhead lines and the assessment of the possibility of adapting current structural solutions for the needs of HSR.

Requirements for the overhead line equipment (OLE) masts are based on typical safety and reliability standards for building structures, covering ultimate limit states (ULS), serviceability limit states (SLS), and fatigue (FAT) under permanent, variable, and potentially seismic loads. The industry standard [5] references the fundamental Eurocodes, including EN 1990, EN 1991, EN 1992, EN 1993 series, etc.

In Poland, it is assumed that the permissible horizontal displacement under variable loads should not exceed 25 mm, which is measured at the height of the running rail (approximately +5.1 m above the railhead). The above requirements must be met by the entire supporting structure system, i.e., the pole along with any connections and foundation elements. Additionally, in Poland, there is also a requirement for the poles to have a smooth surface, meaning that they should not be climbable without additional equipment.

1.2. Column-foundation connections

There are several commonly used methods for connecting OLE masts to the foundation (Fig. 2). One of them is to embed the pole directly into the ground using the so-called smooth connection zone. This is achieved by inserting a suitably longer pole into a drilled hole (Fig. 2c, 2d). It is the most frequently used method for prestressed prefabricated poles and has the advantage of eliminating the need to create and maintain a connection between the pole and the prefabricated foundation. Another method of placing the poles is by fixing them to a monolithic or prefabricated foundation block. At the same time, there are connections between the pole and the foundation with a grout (Fig. 2a) or without it (Fig. 2b). One of the most commonly used solutions in Poland is the so-called “connection with spacing” or “distance connection” (Fig. 2b), which allows for rectification of the pole position, eliminates the problem of water stagnation and corrosion of the column base plates. However, the lack of grout introduces the issue of additional bending of the threaded rods protruding from the foundation and makes it impossible to design a prestressed connection [6].

In such a designed connection (Fig. 2b), tightening the upper nut will at most result in preloading the bolt along the thickness of the base plate.

While the distance-type column-to-foundation connection is commonly used in conventional railway infrastructure, its suit-

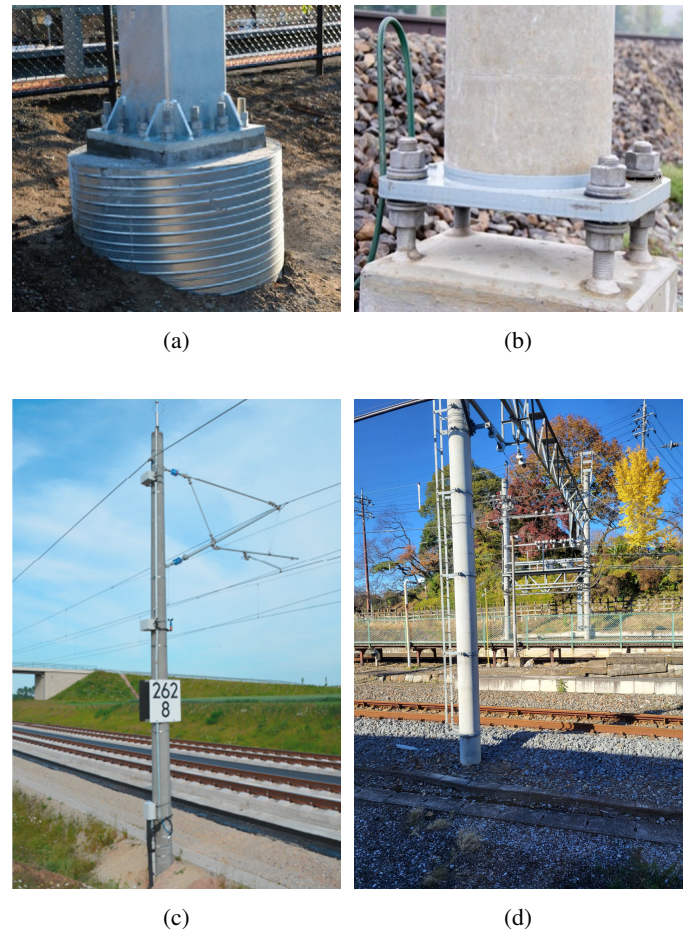


Fig. 2. Common column-base connection examples: (a) On a monolithic foundation with a grout under the base plate – example from Australia (picture [7]), (b) on a prefabricated foundation with a so-called distance connection – example from Poland, (c), (d) column embedded in the ground – examples from Germany (picture [1]) and Japan

ability under the dynamic loading conditions characteristic of HSR remains unverified. In particular, fatigue behavior under train-induced aerodynamic forces has not been sufficiently explored. Furthermore, national experience in HSR design is currently limited, and reliable full-scale measurement data are lacking, which complicates the design verification process. The article aims to analyze the feasibility of adapting the commonly used distance-type connection between the pole and the foundation for application in HSR infrastructure and to identify the range of parameters under which the connection satisfies design requirements. The combined effect of aerodynamic forces induced by high-speed trains and the resultant complex stress state acting upon the connectors necessitates a fatigue analysis of the connectors, as also indicated in [8], to determine the projected fatigue life of the connection.

To clearly define the original contributions of this work, the main original contributions of this study are as follows:

- The first analytical estimation of fatigue performance for distance-type connections subjected to train-induced wind pressure for HSR.

- Confirmation of the susceptibility of the distance-type connection to high-cycle fatigue under train-induced aerodynamic loading.
- Parameterization of aerodynamic loading with Δp and modified S-N curves for bolts M30–M42.
- Drawing attention to the spatial distribution of the load from the passing train on the OLE mast.

2. PROBLEM IDENTIFICATION AND DESCRIPTION

2.1. Wind load on column

In support structures of OLE, cyclic loads occur throughout the entire service life of the railway line. These loads originate from various sources, including wind gusts generated by passing trains, uplift forces from the pantograph, turbulent wind, and vortex-induced vibrations. Each of these loads has a different characteristic (magnitude, direction, distribution) and thus affects the variability of forces in the pole and its anchorage to varying degrees. Heavy poles made from reinforced concrete or prestressed, exhibit a low risk of resonance vibrations, and among the aforementioned factors, the most significant impact comes from wind gusts caused by passing trains, also known as head pressure pulses.

The aerodynamic forces generated by a passing train depend on three key factors: train speed, distance from the train, and train geometry [9, 10]. Among these factors, train speed is of particular significance, as aerodynamic forces increase proportionally to the square of the train velocity [11]. This means that if you consider doubling the allowable speed on a particular railway, a fourfold increase in the passing train loads should be expected. Additionally, the closer an object is to the passing train, the greater the aerodynamic impact [12]. Lastly, the shape of the train nose significantly influences the intensity of the head perturbation. Slender noses (Fig. 1) generate weaker aerodynamic forces compared to bluff-shaped noses.

To add further complexity, two distinct aerodynamic effects occur when a train passes. The first is a pressure pulse generated by the train head, followed by a generally weaker pulse at the tail (Fig. 3). As the train nose moves past, the pressure initially rises sharply, then rapidly drops, all within a very short time. The open-space pressure varies along the length of the train, and for a stationary point located next to the track (such as a column), pressure changes over time will reflect the pressure variations along the train length. These changes show qualitatively similar behavior to those observed on a flat vertical surface [11, 13, 14]. With the difference that the loads from a passing train in open air

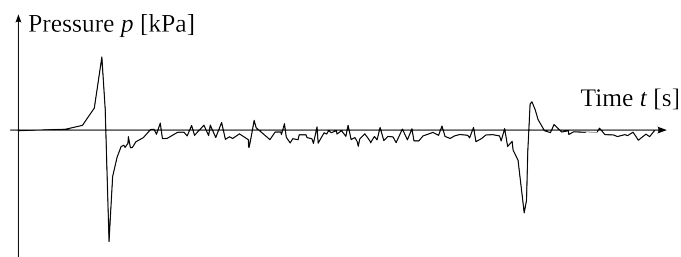


Fig. 3. Time-dependent pressure distribution on a linear element induced by a passing train, developed based on [4]

have a spatial distribution, and taking OLE mast into account, the direction of the load varies from 0 to 360 degrees. The second effect is the airflow induced by the moving train. As the train travels, it creates a boundary layer along its length and a wake behind it. This results in an overall airflow in the direction of the train motion, accompanied by turbulent fluctuations.

Currently, there are no existing HSR lines in Poland, meaning that domestic experience in this field is very limited. Moreover, full-scale measurement data from existing HSR lines are not widely accessible (such as limited to relative values [8]), and even if such data were available, it would be closely tied to the specific characteristics of the locomotives used. Therefore, in this study, the wind pressure value is denoted as Δp and is used as a key parameter for further analysis. It represents the combined effects of gust and turbulence effects caused by a passing train (peak-to-peak value, Fig. 4). Its time distribution follows the model presented in Fig. 3 [4] and corresponds to open-air pressure conditions [8].

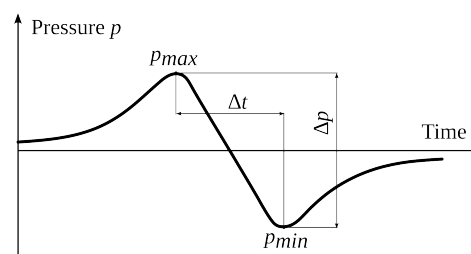


Fig. 4. Peak-to-peak value of the pressure fluctuation induced by the passage of the train nose, as reported in [4]

The magnitude of the generated pressure can be validated using numerical methods such as CFD analysis [15], by calibrating against existing measurement data from operational lines [3, 8] or through experimental studies in wind tunnels [16, 17], analogous to those conducted for sound-absorbing barriers.

2.2. Fatigue strength of steel structures

Each cycle of variable loading causes irreversible damage to the intermolecular bonds within the steel structure, leading to a reduction in tensile, compressive, and shear strength. Over time, this degradation results in a gradual loss of the plastic properties of steel, eventually causing them to disappear entirely. The extent of fatigue crack is gradually increased by the subsequent load repetitions, until finally the effective cross-section is so reduced that catastrophic failure may occur.

Numerous methods for assessing fatigue durability are known [18], which can be categorized into time-based and frequency-based approaches. The traditional approach relies on time-domain analysis using S-N (stress-number of cycles) curves. This curve defines the relationship between stress levels and the number of cycles to failure for a given material. Based on experimental fatigue tests, threshold values are determined, enabling the prediction of the service life of structural components. This method is particularly useful for high-cycle fatigue (HCF) analysis, where stress levels are relatively low, and the dominant damage mechanism is crack propagation within the elastic range.

To estimate the fatigue load-bearing capacity of the column-to-foundation connection, a damage accumulation theory based on frequency-domain analysis was applied. The classical Palmgren-Miner theory assumes a linear summation of fatigue damage, where each cycle at a given stress level $\Delta\sigma_i$ contributes to the progressive deterioration of the material until failure occurs. The core of this method is determining the damage accumulation factor D

$$D = \sum \frac{n_i}{N_i}, \quad (1)$$

where n_i is a number of cycles associated with $\Delta\sigma_i$ for band i in the design histogram, N_i is an endurance (in cycles) obtained for a stress range of $\Delta\sigma_i$, considering the partial factors γ_{Ff} and γ_{Mf} . In EN 1993-1-9, the limit value for the damage sum is indicated as $D_{\max} = 1.0$. It is assumed here that the safety is assured on the actions side, i.e., in the fatigue load models. If the damage accumulation factor D is less than one, the element remains in a serviceable condition.

Fatigue cracks and, consequently, the failure of structural elements are typically initiated at notches (geometric discontinuities, such as threads). The cause of the crack is the stress concentration induced by the notch. A quantitative measure of the notch is the stress concentration factor k_t , which depends on the geometry of the element and the type of loading. It is also emphasized that the k_t parameter does not depend on the load, material, or element size.

3. THESIS

For the purpose of the conducted analyses, the following theses are presented:

- Bending of the threaded rods protruding from the foundation has a significant impact on the stress concentration of the connection.
- Depending on the adopted parameters of the railway line, there is a fatigue issue with the connectors, particularly in the high-cycle fatigue range, which must be considered when designing column-to-foundation connections.
- Only when the load acts perpendicular to the longer side of the base plate are all bolts stressed in the same way. Even a slight change in the load application angle leads to uneven stress distribution in the bolts.
- There is a specific load direction at which the global bending of the column, caused by a passing train, is transferred only by a pair of forces through two connectors.

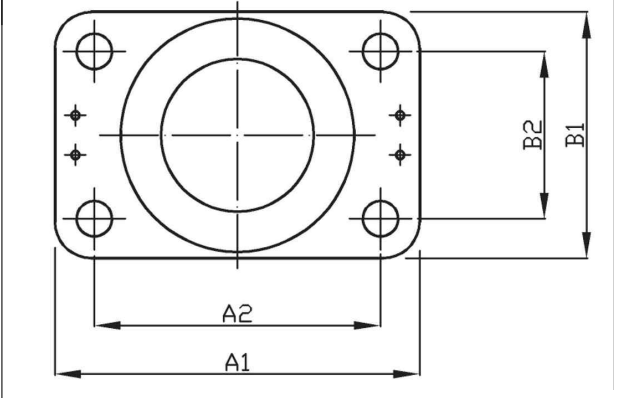
To analyze the impact of the wind gust from a passing train on the fatigue strength of the column-to-foundation connection with a spacing, the following assumptions have been made:

- The geometry of the connection to pole foundations PI, PII, and PIII, as shown in Table 1.
- The columns subjected to the load from the passing train, corresponding to the PI, PII, and PIII connections, have a top diameter of 177 mm, 233 mm, and 233 mm, respectively, and a height of 8.2 m above the top of the rail.
- The railway line load is assumed to be 100 train passes per day.

At this stage, it is assumed that one train passage corresponds to a single fatigue cycle, which means that wind fluctuations along the train (Fig. 3), as well as the intensified pulse occurring after the train tail passes, were omitted.

Table 1
Geometry of the connection

Connectors	Poles		
	PI	PII	PIII
Size	M30	M36	M42
Spacing A2 × B2	320 × 190	385 × 225	435 × 255



4. CONFIRMATION OF ASSUMPTIONS THROUGH ANALYTICAL CALCULATIONS

4.1. Stress state in a single connector

The pressure value is represented by the parameter Δp [kPa]. The dynamic response of the column geometry is accounted for by the aerodynamic resistance coefficient with the influence of the free-end flow c_f , and the structural parameter $c_s c_d$, which are 0.589 and 2.095, respectively. The load defined in this way has a distribution as shown in Fig. 5, with values $q_{\text{top}} = 0.469\Delta p$, $q_{\text{bottom}} = 0.636\Delta p$ for a column with a top diameter of 177 mm, and $q_{\text{top}} = 0.595\Delta p$, $q_{\text{bottom}} = 0.762\Delta p$ for columns with a top diameter of 233 mm. For the purpose of the analysis, the loading area of the column below the railhead was omitted.

The values of the bending moment M and shear force V resulting from the static equilibrium of the system are presented in Table 2. At this stage, a simplification is made, and the influence of the loading application time on the static equilibrium is not considered. It is acknowledged that accounting for dynamic amplification due to the impulsive nature and rapid alternating sign

Table 2
Forces at the base of the column

	PI	PII	PIII
M	$9.32\Delta p$	$11.52\Delta p$	$11.52\Delta p$
V	$2.762\Delta p$	$3.392\Delta p$	$3.392\Delta p$

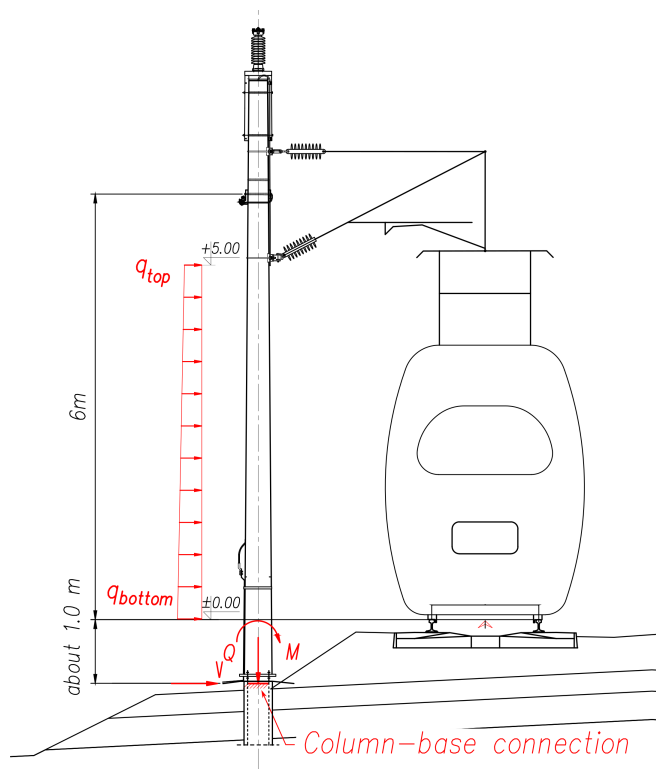


Fig. 5. Common column-base connection examples

of the applied excitation could increase the forces determined under static assumptions. It is assumed that the load application time is similar to typical gusts of wind, in accordance with [12].

Considering the geometry of the base plate and the distance of approximately $c = 10$ cm between the base plate of the column and the upper part of the foundation, the forces in a single connector due to the passing train are presented in Table 3. Whereas F_H is a shear force in a single connector, F_Q is an axial force in a single connector, and M is a bending moment in a single connector, calculated as $M = F_H c$. Based on these forces, the stress amplitude $\Delta\sigma_R$ was determined, defined as the sum of the axial stress $\Delta\sigma_N$ and the bending stress $\Delta\sigma_M$ in the connector.

Table 3

Internal forces and stresses in a single connector

	PI	PII	PIII
F_H	$0.691\Delta p$	$0.848\Delta p$	$0.848\Delta p$
F_Q	$14.56\Delta p$	$14.97\Delta p$	$13.25\Delta p$
M	$0.069\Delta p$	$0.085\Delta p$	$0.085\Delta p$
$\Delta\sigma_N$	$26.0\Delta p$	$18.3\Delta p$	$11.8\Delta p$
$\Delta\sigma_M$	$36.9\Delta p$	$25.8\Delta p$	$16.0\Delta p$
$\Delta\sigma_R$	$62.9\Delta p$	$44.1\Delta p$	$27.8\Delta p$

In the adjustable, distance connection, the connectors are additionally subjected to bending due to the horizontal force and the distance between the base plate and the pile top surface.

The bending stresses represent a significant portion of the stress amplitude $\Delta\sigma_R$, i.e., over 55% of the total stress (Table 3).

4.2. Fatigue life

The normative fatigue strength was calculated based on [19], appropriate for a threaded element. The scale effect and the partial factor for the unconditional life method with significant destruction consequences $\gamma_{Mf} = 1.35$ were considered, determining the computational limiting value of the stress amplitude $\Delta\sigma_c$ [20]. It corresponds to typical detail categories for fatigue strength of 2 million cycles. The design value of the limiting stress amplitude in a single connector M42 is

$$\Delta\sigma_{C,M42} = \frac{50}{1.35} 0.92 = 34.0 \text{ MPa} \quad (2)$$

For M30 and M36 threaded elements, the $\Delta\sigma_c$ is 37.0 MPa and 35.4 MPa, respectively.

In addition to the limited fatigue strength $\Delta\sigma_c$, it is also possible to determine a range of variable stresses for which fatigue does not occur. This results in a solution referred to as the so-called “permanent fatigue strength”, which is understood as the largest stress amplitude at which the element does not fail, regardless of the number of cycles. The permanent fatigue strength is determined by considering the limiting stress amplitude, further reduced by a coefficient of 0.737, and is calculated as: $\Delta\sigma_{D,M42} = 0.737\Delta\sigma_c = 25.1$ MPa. For M30 and M36 threaded elements, the $\Delta\sigma_D$ is 27.3 MPa and 26.1 MPa, respectively.

Based on the fatigue strength, the service life of the connection N_R , expressed as the number of cycles of stress with a constant amplitude, is determined [20]. This value is calculated based on the reduced Wöhler curve. For nominal stress spectra with stress ranges above and below the constant amplitude fatigue limit D , the fatigue strength should be based on the extended fatigue strength curves as follows:

$$\Delta\sigma_R^m \cdot N_R = \Delta\sigma_C^m \cdot 2 \cdot 10^6 \quad \text{with } m = 3 \text{ for } N < 5 \cdot 10^6 \quad (3)$$

$$\Delta\sigma_R^m \cdot N_R = \Delta\sigma_D^m \cdot 5 \cdot 10^6 \quad \text{with } m = 5 \text{ for } 5 \cdot 10^6 \leq N \leq 10^8, \quad (4)$$

where $\Delta\sigma_R$ is a stress amplitude in an element, N_R is a design lifetime expressed as the number of cycles related to a constant stress range, $\Delta\sigma_c$ or $\Delta\sigma_D$ is a reduced reference value of the fatigue strength, m is the slope of the fatigue strength curve.

For the assumptions made, with wind acting in a direction perpendicular to the railway line (on the strong axis of the base plate of the column) and the variation of the parameter Δp in the range from 0.5 to 1.6 kPa, the fatigue curves are presented in Fig. 6 and the calculation summary in Table 4.

An addition to the determined curves is the value of the damage accumulation degree D for the connection (Fig. 7). It was used for predicting the fatigue life by assuming a 50-year service life of the solution (i.e., $50 \cdot 36500 = 1.825 \cdot 10^6$ cycles).

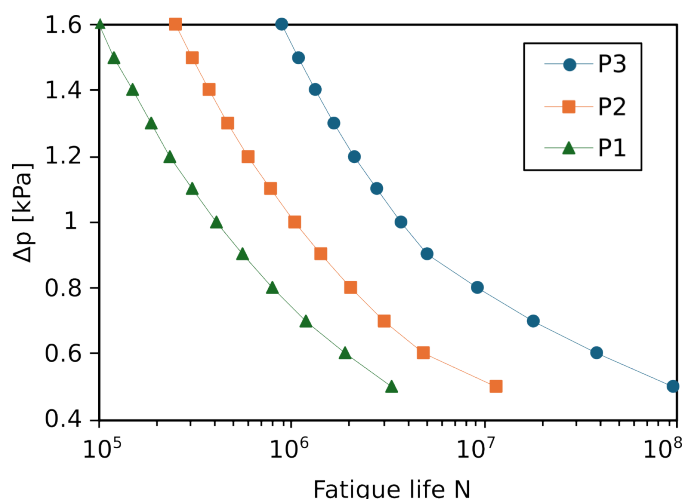


Fig. 6. Modified S-N curves for different Δp values

Table 4

Fatigue life estimation when wind acts on the strong axis of the base plate of the column

		PI	PII	PIII
Fatigue life for $N < 5 \cdot 10^6$	$N \cdot 10^5$	$4.09\Delta p^{-3}$	$10.3\Delta p^{-3}$	$36.6\Delta p^{-3}$
Fatigue life for $5 \cdot 10^6 \leq N \leq 10^8$	$N \cdot 10^5$	$0.772\Delta p^{-5}$	$3.62\Delta p^{-5}$	$29.8\Delta p^{-5}$

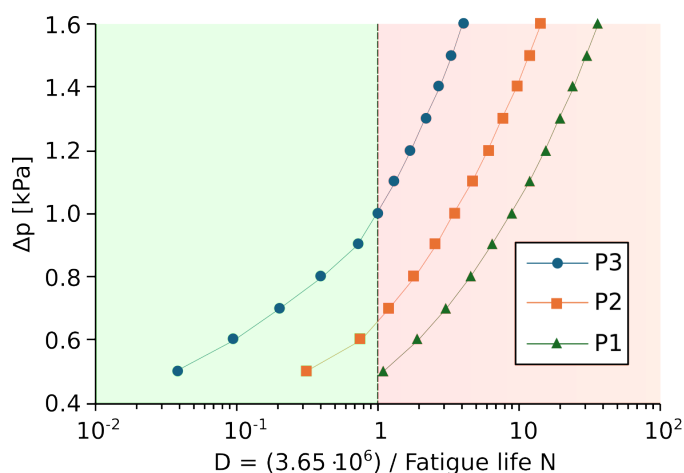


Fig. 7. Relationship between the damage accumulation degree D and different values of the wind pressure Δp

For the area where the damage accumulation degree is less than one, the fatigue strength will not be exceeded within the assumed service life. This means that the connection will retain its fatigue strength and will not fail due to fatigue damage during the designated period.

4.3. Additional analysis

The load from the passing train is a complex issue exhibits variable and unpredictable characteristics such as gusts and tur-

bulence. Without going into detailed calculations, the passing train alters the wind direction (i.e., the position of the neutral axis relative to which the load is applied), and assuming that the load value remains unchanged, the following scenario arises: The neutral axis rotates from its initial position, from the blue axis which is parallel to the track, to a new position marked in red (Fig. 8), passing through two of the four bolts. As a result, the assumption of an equal distribution of the bending load across the four bolts becomes incorrect. It is then necessary to consider that the bending moment is carried only by the two bolts working on a $2 \cdot 219 = 438$ mm arm, appropriate to PIII poles (Fig. 8).

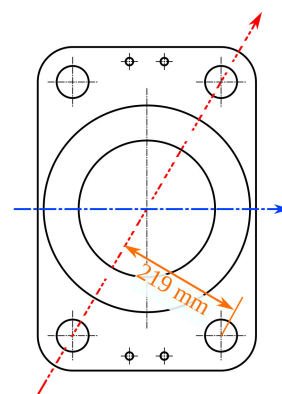


Fig. 8. Layout of a steel column base PIII with an unfavorable position of the neutral axis when bending (red axis)

The most unfavorable angle of load application limits the contribution to the bending transfer to only two bolts. The calculations performed are summarized in Table 5. The results of the unfavorable force configuration, assuming the variability of the parameter Δp , ranging from 0.3 kPa to 1.6 kPa are presented in Fig. 9.

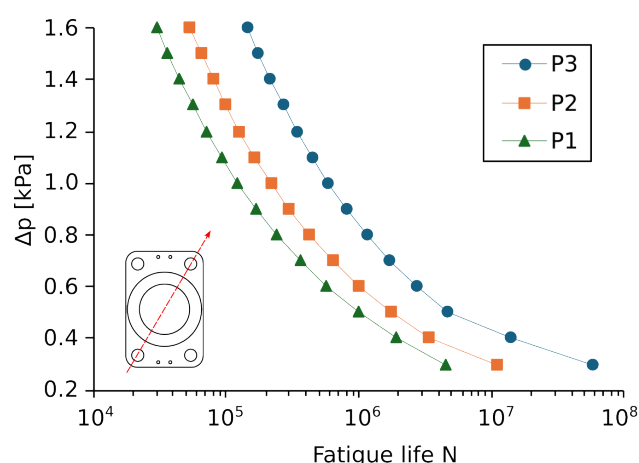


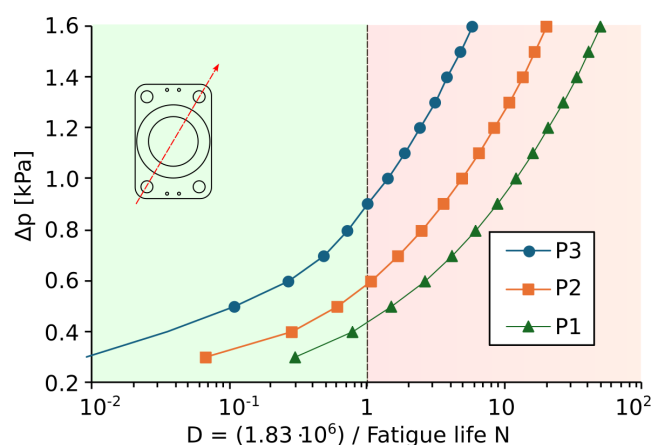
Fig. 9. Modified S-N curves assuming the most unfavorable wind pressure direction

The determination of the damage accumulation degree for the unfavorable direction further emphasizes the system sensitivity to the direction of the applied load (Fig. 10).

Table 5

Summary of calculations for the most unfavorable angle of wind load

		PI	PII	PIII
Wind load at the top	q_{top}	$0.47\Delta p$	$0.59\Delta p$	$0.59\Delta p$
Wind load at the bottom	q_{bottom}	$0.64\Delta p$	$0.76\Delta p$	$0.76\Delta p$
Moment at the base of the column	M	$9.32\Delta p$	$11.5\Delta p$	$11.5\Delta p$
The distance between the neutral axis and the single bolt	z	0.163	0.194	0.219
Axial force in the bolt	F_Q	$28.5\Delta p$	$29.7\Delta p$	$26.2\Delta p$
Shear force in one bolt	F_H	$0.69\Delta p$	$0.85\Delta p$	$0.85\Delta p$
Moment of horizontal force	M	$0.07\Delta p$	$0.08\Delta p$	$0.08\Delta p$
Size of the bolt	–	M30	M36	M42
Stresses from axial force	σ_N	$50.9\Delta p$	$36.3\Delta p$	$23.4\Delta p$
Stresses from bending in the bolt	σ_W	$36.9\Delta p$	$25.8\Delta p$	$16.0\Delta p$
Stress amplitude in the bolt	$\Delta\sigma_R$	$87.8\Delta p$	$62.1\Delta p$	$39.4\Delta p$
Fatigue life for $N < 5 \cdot 10^6$	$N \cdot 10^5$	$1.50\Delta p^{-3}$	$3.70\Delta p^{-3}$	$12.9\Delta p^{-3}$
Fatigue life for $5 \cdot 10^6 \leq N \leq 10^8$	$N \cdot 10^5$	$0.145\Delta p^{-5}$	$0.654\Delta p^{-5}$	$5.25\Delta p^{-5}$

**Fig. 10.** The relationship between the damage accumulation degree D and the wind pressure Δp , assuming the most unfavorable wind pressure direction

5. FUTURE RESEARCH

Future efforts may include wind tunnel testing, in-depth CFD simulations, and validation using measurements from existing tracks to enhance the understanding of system performance and optimize design solutions. Such an approach will facilitate the

identification of variations in load direction and the assessment of pressure magnitudes and their vertical distribution along the pole induced by passing trains. Therefore, more advanced analyses should be conducted with respect to both wind effects and fatigue strength. This includes, among others, modal analysis of the system, aerodynamic coupling, interaction with gusts, and identification of other factors causing cyclic loading of OLE masts. Additionally, fatigue behavior of the connectors should be examined, taking into account aging, local material degradation, and potential bolt slippage. On the other hand, given the rapid development of HSR in Poland, there is a clear need for full-scale experimental testing to verify the magnitude and distribution of loads generated by passing trains under realistic operating conditions - not only for the connection itself, but for the entire OLE system.

6. CONCLUSIONS

The article presents considerations regarding the fatigue life of connections with spacing between a column and a foundation, highlighting the design challenge stemming from the difficulty of estimating the wind pressure generated by a passing train. The design of OLE masts for HSR infrastructure is a complex engineering task influenced by wind action, dynamic effects, and power supply system requirements. At the current stage of HSR development in Poland, the lack of interdisciplinary coordination complicates the design process significantly. Effective information exchange is essential for accurate and cost-efficient design. Given the current findings, numerous simplifications are necessary. For this reason, the aerodynamic load was introduced as a simplified parameter (Δp), among others, and a series of parametric analyses was carried out.

The fatigue strength of the pile connectors was determined, and parametric fatigue strength calculations were conducted. The results are presented in graphical form to enhance clarity and support further analysis.

These findings reveal important trends and design implications, including:

1. An analysis of the fatigue damage spectrum was conducted, based on which it is concluded that, depending on the adopted track parameters, there is an issue with the fatigue of the connectors when the distance connection is designed.
2. The distance connection is unable to prestress connectors, making them susceptible to fatigue cracking. Additional bending of the connectors between the base plate of the column and the upper part of the foundation further strains the connectors and limits the durability of the system. The bending stresses represent over 55% of the total stress amplitude $\Delta\sigma_R$.
3. The connection is sensitive to boundary conditions, particularly to the angle of action of the wind on the structure. Even with a small deviation from the perpendicular angle (i.e., acting on the strong axis of the base plate), the wind also acts on the column in such a way that the neutral bending axis passes through two connectors. In this case, only two out of the four connectors transfer the bending moment induced by the passing train. This is the most unfavorable load

direction, in which the reduction in the fatigue life of the connection reaches approximately $(36.6-12.9)/36.6 = 65\%$ for configuration PIII.

The main motivation of this study was to gain a better understanding of the fatigue life of the adjustable column-to-foundation connection. The paper presents results that provide valuable insights for future research, particularly concerning the potential adaptation of this commonly used connection type in Poland for OLE masts in HSR systems.

REFERENCES

- [1] F. Alkam and T. Lahmer, "A robust method of the status monitoring of catenary poles installed along high-speed electrified train tracks," *Results Eng.*, vol. 12, p. 100289, 2021, doi: [10.1016/j.rineng.2021.100289](https://doi.org/10.1016/j.rineng.2021.100289).
- [2] W. Powrie, D.J. Richards, and V.K.S. Mootoosamy, "The design of railway overhead line equipment mast foundations," *Proc. Inst. Civ. Eng.-Geotech. Eng.*, vol. 173, no. 5, pp. 428–447, 2019, doi: [10.1680/jgeen.18.00242](https://doi.org/10.1680/jgeen.18.00242).
- [3] D.J. Richards, W. Powrie, and A.P. Blake, "Full-scale tests on laterally loaded railway overhead line equipment mast foundations," *Géotechnique*, vol. 73, no. 3, pp. 189–201, 2023, doi: [10.1680/jgeot.20.P.312](https://doi.org/10.1680/jgeot.20.P.312).
- [4] European Committee for Standardization, "EN 14067-4:2024 Railway applications – Aerodynamics – Part 4: Requirements and assessment procedures for aerodynamics on open track". 2024.
- [5] European Committee for Standardization, "PN-EN 50119:2020 Railway applications: Fixed installations. Electric traction overhead contact lines".
- [6] W.-Y. Lim, D. Lee, and Y.-C. You, "Exposed column-base plate strong-axis connections for small-size steel construction," *J. Construct. Steel Res.*, vol. 137, pp. 286–296, 2017, doi: [10.1016/j.jcsr.2017.06.018](https://doi.org/10.1016/j.jcsr.2017.06.018).
- [7] B. Hu and R.W.K. Chan, "Railway Overhead Wiring Structures in Australia: Review and Structural Assessment," *Appl. Sci.*, vol. 12, no. 3, 2022, doi: [10.3390/app12031492](https://doi.org/10.3390/app12031492).
- [8] D. Rocchi, G. Tomasini, P. Schito, and C. Somaschini, "Wind effects induced by high speed train pass-by in open air," *J. Wind Eng. Ind. Aerodyn.*, vol. 173, pp. 279–288, 2018, doi: [10.1016/j.jweia.2017.10.020](https://doi.org/10.1016/j.jweia.2017.10.020).
- [9] P. Derkowski *et al.*, "High-speed rail aerodynamic assessment and mitigation report: final report," US Department of Transportation. Federal Railroad Administration. Office of Research, Development, and Technology, DOT/FRA/ORD-15/40, Dec. 2015. [Online]. Available: https://rosap.nrl.bts.gov/view/dot/31176/dot_31176_DS1.pdf
- [10] H. Shui-Hong Lee, "Safety of High-Speed Ground Transportation Systems: Assessment of Potential Aerodynamic Effects on Personnel and Equipment in Proximity to High-Speed Train Operations," US Department of Transportation. Federal Railroad Administration. Office of Research and Development, DOT-VNTSC-FRA-98-3; DOT/FRA/ORD-99/11;, Dec. 1999. [Online]. Available: <https://rosap.nrl.bts.gov/view/dot/8446>
- [11] D. Liu, C. Wang, J. Gonzalez-Libreros, Y. Tu, L. Elfgren, and G. Sas, "A review on aerodynamic load and dynamic behavior of railway noise barriers when high-speed trains pass," *J. Wind Eng. Ind. Aerodyn.*, vol. 239, p. 105458, 2023, doi: [10.1016/j.jweia.2023.105458](https://doi.org/10.1016/j.jweia.2023.105458).
- [12] European Committee for Standardization, "EN 1991-1-4:2005 Eurocode 1: Actions on structures. Part 1-4: Wind Actions".
- [13] Y. Sakuma, T. Nakano, T. Inoue, and Y. Kakizaki, "Wind loads on flat plates and porous screens installed on the track surface during the passage of high-speed trains," *J. Wind Eng. Ind. Aerodyn.*, vol. 256, p. 105951, 2025, doi: [10.1016/j.jweia.2024.105951](https://doi.org/10.1016/j.jweia.2024.105951).
- [14] H. Liang, Y. Zou, D. Guo, C. Cai, and X. He, "Analysis of concrete damage at anchorage end of the high-speed railway bridge sound barrier under the 400 km/h train-induced wind loads," *Structures*, vol. 69, p. 107284, 2024, doi: [10.1016/j.istruc.2024.107284](https://doi.org/10.1016/j.istruc.2024.107284).
- [15] Y.-K. Tan, D.-H. Ouyang, E. Deng, H. Yue, and Y.-Q. Ni, "CFD-guided memory-enhanced LSTM predicts leeward flow of railway windproof structures," *Adv. Eng. Inform.*, vol. 65, p. 103253, 2025, doi: [10.1016/j.aei.2025.103253](https://doi.org/10.1016/j.aei.2025.103253).
- [16] J. Zhang, M. Zhang, Y. Li, and C. Fang, "Aerodynamic effects of subgrade-tunnel transition on high-speed railway by wind tunnel tests," *Wind Struct. Int. J.*, vol. 28, pp. 203–213, Apr. 2019, doi: [10.12989/was.2019.28.4.203](https://doi.org/10.12989/was.2019.28.4.203).
- [17] S.A. Hashmi, H. Hemida, and D. Soper, "Wind tunnel testing on a train model subjected to crosswinds with different windbreak walls," *J. Wind Eng. Ind. Aerodyn.*, vol. 195, p. 104013, 2019, doi: [10.1016/j.jweia.2019.104013](https://doi.org/10.1016/j.jweia.2019.104013).
- [18] L. Zhang *et al.*, "Methods for fatigue-life estimation: A review of the current status and future trends," *Nanotechnol. Precis. Eng.*, vol. 6, no. 2, p. 025001, Feb. 2023, doi: [10.1063/1.50017255](https://doi.org/10.1063/1.50017255).
- [19] European Committee for Standardization, "EN 1993-1-9:2007 Eurocode 3: Design of steel structures. Part 1-9: Fatigue".
- [20] A. Nussbaumer, L. Borges, and L. Davaine, "Fatigue Design of Steel and Composite Structures: Eurocode 3: Design of Steel Structures Part 1-9 – Fatigue/Eurocode 4: Design of Composite Steel and Concrete Structures," in *Fatigue Design of Steel and Composite Structures*, John Wiley & Sons, Ltd, 2018, pp. 157–182. doi: [10.1002/9783433608791](https://doi.org/10.1002/9783433608791).